Solar Steel Sandwich Panels for Industrial and Commercial Buildings: System Simulations and Potential Analysis

Finn Weiland, Maik Kirchner, Fabian Hüsing, Federico Giovannetti

Institute for Solar Energy Research in Hamelin (ISFH), Emmerthal (Germany)

Abstract

Building integration can improve the architectural and aesthetical quality of solar installations and reduce their cost. The development and performance assessment of solar steel sandwich panels for the use in industrial and commercial buildings have been already demonstrated in previous works. The present paper analyses the behavior of the panels for the assistance of ground-coupled heat pump systems by means of simulations with TRNSYS, focusing on the energetic regeneration of the geothermal source. The results show that the combination with solar panels can slightly improve the energy performance of well-designed systems (+5%), but significantly affects the efficiency of systems with undersized borehole heat exchangers. Solar regeneration enables to reduce the length or the number of the boreholes by 25 % to 30 % and the area necessary for their installation up to 80 %.

Keywords: heat pump system, solar collector, solar regeneration, building integration, sandwich panel

1. Introduction

The research project "Building-integrated solar steel sandwich elements for industrial and commercial buildings with a mineral wool core" aims at the solar thermal use of sandwich façades to supply heat to non-residential buildings. Steel sandwich panels are well-established components for the cost-effective manufacturing of functional envelopes in commercial and industrial buildings. They can be adapted for the active use of solar energy by integrating suitable heat exchangers between the front cladding and the insulating core, as already shown in previous works (Fig. 1, left). Weiland et al. (2019) show the performance potential of different absorber geometries in FEM simulation studies validated by measurements. On the basis of these results, large-format prototypes with heat exchangers consisting of meander tube registers with heat transfer plates were manufactured in the project. The performance of first demonstrators has been determined by means of indoor and outdoor measurements (ISO 9806, 2018). For large-sized prototypes (2 m²) with a grey coating (solar absorptance = 0.865, according to ISO 9050) and 70% activation of the total surface we reported zero-loss thermal efficiencies η_0 up to 0.56. Calculations based on validated FEM-models (Fig. 1, bottom right) estimate maximum values up to 75%.

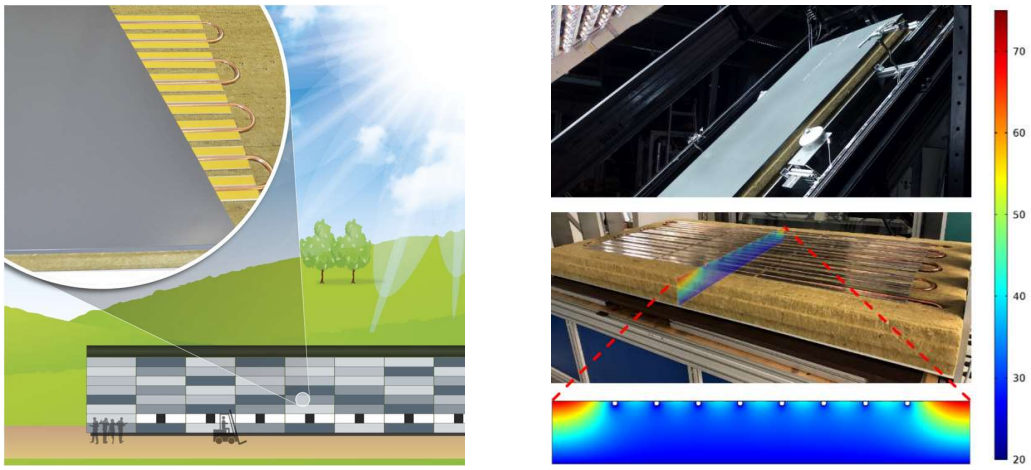

Fig. 1: Exemplary visualization of building integrated solar panels with detail of the developed prototype (left) and a prototype in the sun simulator (top right), with a temperature field of the validated FEM simulations (in degrees Celsius) (bottom right).

Selection and/or peer review under responsibility of Scientific Committee
doi:10.18086/eurosun.2020.01.14 Available at http://proceedings.ises.org

The aim of the simulation studies presented in this paper is to investigate the behavior of the developed sandwich panels in systems and their potential for supplying heat to industrial and commercial buildings. The solar-activated panels correspond in their design to uncovered thermal collectors and have a relatively high heat loss coefficient. They supply heat mainly at ambient temperature level (< 40° C) and are thus optimally suited for combination with ground-coupled heat pump systems. The focus of the work is on their combination with brine-to-water heat pumps and on their potential to regenerate the geothermal source. The regeneration not only offers the opportunity to increase the efficiency and robustness of the systems, but is also a prerequisite for ensuring their sustainable operation. For regeneration, various measures can be considered, with solar thermal energy being a reasonable and proven option. Extensive studies on this topic have already been carried out in previous works (Bertram et al., 2014; Hadorn, 2015; Persdorf et al., 2015).

2. Boundary conditions of the Simulation studies

The simulations are carried out with the software TRNSYS. The transient system simulation software TRNSYS (version 17) is mainly used for the modelling of multi-zone buildings and heating systems in dynamic annual simulations (Transsolar Energietechnik, 2012). The following section describes the boundary conditions of the simulations, parameter variations and sensitivity analyses.

2.1. Heat demand: Building model and usage profiles

The thermal energy is provided for an exemplary building with a floor area of 900 m², which is heated by an industrial floor heating system. The basic dimensions are shown in figure 3. The specifications of the outer shell are described in Feldmann et al. (2014) and are adapted to the requirements of the current energy saving directive (EnEV, 2016). Decisive for the selection of components is the maximum value of the heat transfer coefficient for non-residential buildings. Relevant are the key figures for enclosing building components such as exterior walls and roofs (U = 0.35 W/m²K). Accordingly, construction-relevant, marketable steel sandwich elements with a mineral wool core and an insulation thickness of 120 mm were selected. The natural lighting of the building is provided by a 50 m long ridge light band.

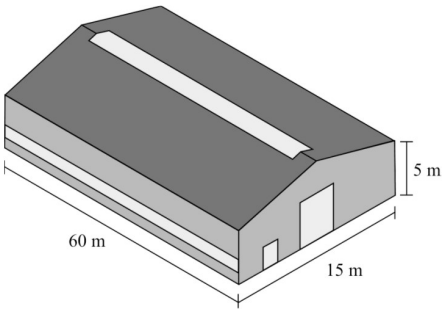

Fig. 2: Schematic representation (left) and supporting structure (right) of the investigated building

The reference document for the energy evaluation of buildings is the DIN V 18599 (2018), which specifies compliance with the energy requirements according to EnEV and takes into account compliance with the EEWärmeG (2008). Oschatz et al. (2015) provide a good overview of the requirements for non-residential buildings in this context. There are essentially three activity levels for activities in commercial and industrial buildings and associated minimum requirements for the target room temperature and the minimum air change rate. The requirements for the room temperature are also defined by the technical workplace regulation (BAuA, 2018). The scenarios used in the simulations are chosen in accordance with the relevant standards. For the studies in this paper, a scenario for a production hall heated to 19 °C target temperature is selected. Within the building, a two-shift operation with light work (standing or walking) with internal gains of 39 W/m² for duration of occupancy is simulated. The provision of hot drinking water is not considered due to the varying loads in commercial and industrial scenarios. Besides a continuous natural infiltration of 0.14 h^{-1}, an air exchange rate through ventilation of 0.60 h^{-1} is assumed when the building is occupied. The internal gains are calculated according to DIN V 18599 over an average occupancy density. The resulting heat demand for the location Zurich (Meteonorm, 2015) is 82.9 MWh/a, which corresponds to a specific heat demand of 92.1 kWh/(m²a). The floor heating is designed for a flow temperature of 35 °C, a return flow temperature of 30 °C and has a specific heating power of 57 W/m². 600 m² of the floor area are activated, which corresponds to a total heating power of 34.2 kW.

2.2. System configuration

In order to demonstrate the effects of the solar use of steel sandwich façades, we have defined two heat pump systems for comparison. The main reference system is a brine-water heat pump system (55.8 kW at B0/W35, COP = 4.81), in which borehole heat exchanger (a field of geothermal probes) serves as a heat source for the heat pump. In the case of solar regeneration, this reference system is extended by a field of solar-activated steel sandwich elements on the south façade of the building. In addition, the results are compared with an air-to-water heat pump system (65.1 kW at A2/W35, COP = 3.60), where the ambient air serves as heat source for the heat pump. In each system, a buffer tank is connected between the heat pump and the underfloor heating system to avoid frequent clocking and thus minimize the number of heat pump starts. The storage tank is also used in practice with air-water heat pumps to provide the necessary energy for defrosting. For the sake of simplicity, these defrosting operations are not taken into account in the simulations. The three systems are schematically shown without the buffer storage tanks in Figure 3:

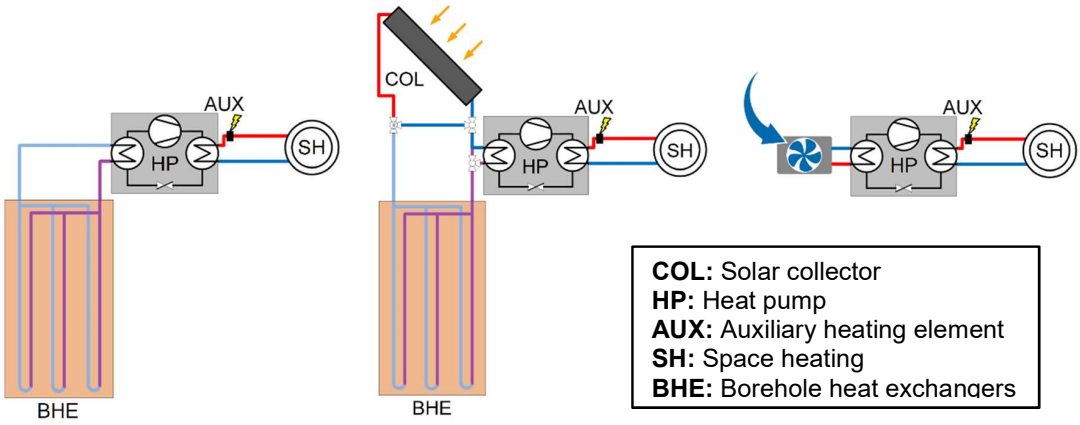

Fig. 3: Schematic representation of the system configurations examined: Brine-water heat pump with borehole heat exchanger without (left) and with solar thermal regeneration (middle) and air-to-water heat pump (right)

The regeneration of the borehole heat exchanger takes place as soon as the outlet temperature of the collector field exceeds the outlet temperature of the borehole field by 5 K. The collector circuit comes to a standstill again when the collector outlet temperature falls below the outlet temperature of the borehole heat exchanger.

2.3. Heat pump source: Geothermal borehole heat exchanger

The source of the heat pump system consists of a field of geothermal probes, each 100 m long. The upper 2 m are thermally insulated (frost protection) and the rest is effectively used for heat exchange with the ground. The probes are arranged in a rectangular area with a distance of 10 m each. The number of probes is set as a simulation parameter to investigate the influence of the size of the field on the system performance. The number and arrangement of the probes shown in the following table are selected for the simulation study:

Tab. 1: Investigated number and arrangement of the boreholes in the probe field in the parameter study

Quantity	Arrangement	Total length	Surface area
6	2 x 3	600 m	200 m²
9	3 x 3	900 m	400 m²
12	3 x 4	1200 m	600 m²
16	4 x 4	1600 m	900 m²

For the soil properties, a normal to poor subsoil with a thermal conductivity of $\lambda = 1.52$ W/(m*K) is assumed in accordance with VDI 6440-2 (2019), which corresponds to a heat extraction rate of 35 W/m. In order to ensure a sustainable operation of the borehole heat exchanger, the simulation period is set to 25 years and the minimum inlet temperature of the probe field was limited to -3 °C in order to avoid frost conditions in the filling material (SIA, 2010). In addition, the inlet temperature in the case of solar regeneration is limited to a maximum of 25 °C in order to meet the sustainability criteria.

2.3. Solar activated steel sandwich panels

The characteristic values of the sandwich collectors used in the simulations correspond to the characteristic values of a prototype measured in the sun simulator according to ISO 9806 (2018). The conversion factor η_0 is 53.3 % and the absorption coefficient α is 86.5 % (RAL 7012). The linear loss coefficient b_1 is 8.9 W/(m²K) and the wind-dependent coefficients b_2 and b_u are 1.37 J/(m³K) and 0.057 s/m respectively (Weiland et al., 2019). The efficiency η of the collector can be calculated with these characteristic values, depending on the wind speed v. The efficiency also depends on the temperature difference between ambient and fluid temperature T_{fl} - T_a, divided by the standardized irradiance E_N. This term is also called $Tm*$.

$$\eta = \eta_0 * (1 - b_u * v) - (b_1 + b_2 * v) * \frac{T_{fl} - T_a}{E_N} \qquad \text{(eq. 1)}$$

When calculating the normalized irradiance E_N, the radiant heat losses are taken into account or compensated for if the sky temperature deviates from the ambient temperature. The collector characteristic curves are shown in Figure 4 for three different wind speeds.

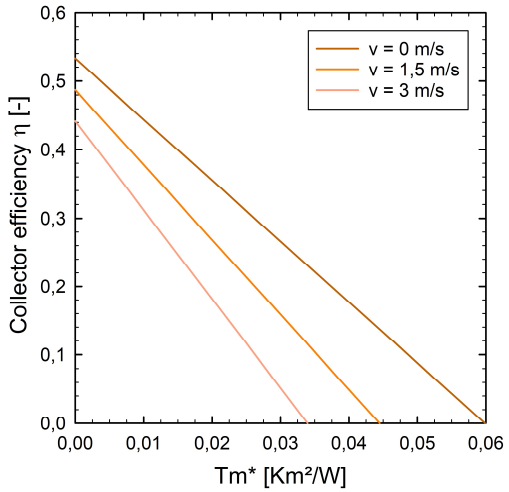

Fig. 4: Efficiency curve of the collector at different wind speeds

The effective capacity c_{eff} of the collector is calculated according to ISO 9806 (2018) and is 16.5 kJ/(m²K). In a parameter study, the area of the solar-activated façade is varied between 60 m² and 120 m². In a further parameter study, the solar absorptance of the cover shell is varied to take into account the influence of differently colored surfaces. In addition to the color RAL 7012 (α = 86.5 %), the following grey shades commonly used for commercial building envelopes are considered: RAL 9006 (α = 52.8 %), RAL 9007 (α = 76.2 %), and RAL 7016 (α = 91.3 %). The collector characteristics correspondent to these color variations are calculated with a stationary collector model developed at ISFH (Föste, 2013).

2.3. Evaluation criteria

The energy evaluation is based on the Seasonal Performance Factor (SPF) calculated at the end of the simulation period (25 years of operation). The selected evaluation boundary is decisive for this criterion. In the frame of the IEA TASK 44, Malenković et al. (2013) give an overview of the different evaluation boundaries and their suitability for the comparison of different heat supply systems with heat pumps. The SHP+ boundary covers all electrical consumers of the heat supply system so that different supply systems can be compared very well with each other at identical load profiles and temperatures. The system annual performance factor SPF_{SHP+} is therefore selected for our assessment. It is defined as the ratio of the heat provided by the room heating Q_{RH} to the total electrical work W_{total} required. This consists of the respective work of the heat pump W_{WP}, of the circulation pumps W_{CP}, of the electrical heater W_{EH} and the auxiliary energy W_{Aux}:

$$SPF_{SHP+} = \frac{Q_{RH}}{W_{total}} = \frac{Q_{RH}}{W_{HP}+W_{CP}+W_{EH}+W_{Aux}} \qquad \text{(eq. 2)}$$

Another decisive factor for the efficiency of the system is the bivalence point, the minimum inlet temperature of the ground heat exchanger fluid. Since it is limited to -3 °C, an electrical heater takes over the heat supply if this temperature falls below this value.

3. Results of the energetic analysis

The results show that the ground-coupled systems achieve a very high efficiency. For example with a probe length of 1200 m, the SPF_{SHP+} slightly improves from 4.50 (reference system) to 4.74 by regenerating the borehole heat exchanger with solar-thermally activated sandwich elements. The significantly greater effect, however, is achieved with a tightly dimensioned geothermal heat source due to the possibility of reducing the borehole length. By using 120 m² sandwich elements, the length can be reduced by 25 % to 30 % with the same energetic performance. To illustrate these results, Figure 5 shows the SPF_{SHP+} (left) and the minimum fluid inlet temperature (right) after an operating time of 25 years:

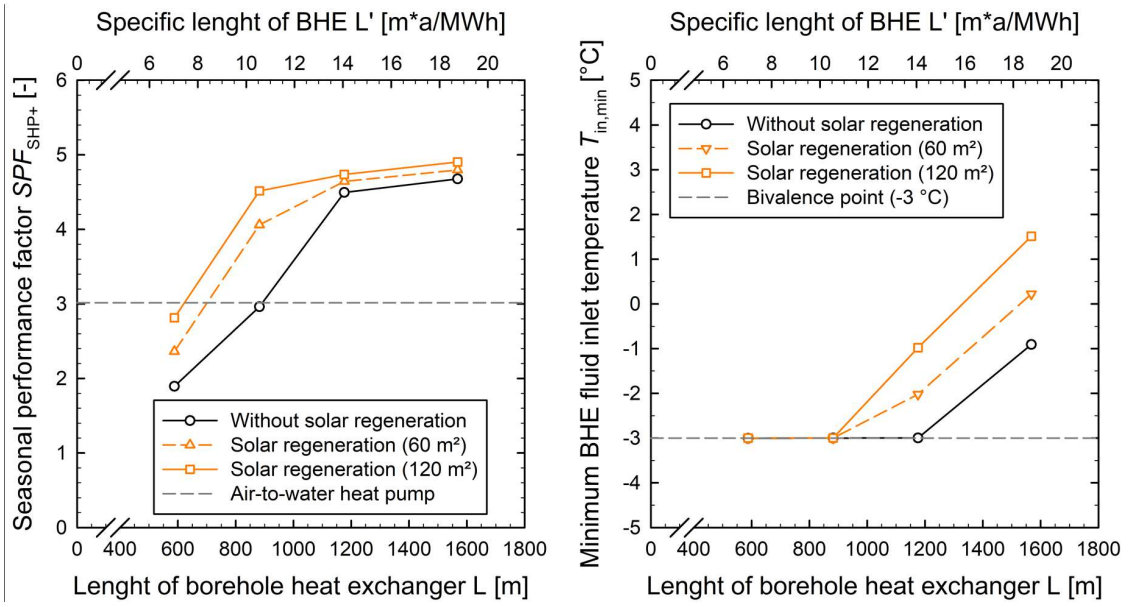

Fig. 5: Seasonal performance factor (left) and minimum fluid inlet temperature into the probe field after 25 years of operation.

The results with an air-to-water heat pump as the heat generator show that this simpler system is about 35% less efficient and thus consumes 35% more electricity than the ground-couple one. Furthermore, the seasonal differences in the efficiency are significantly higher than that. Accordingly, if the source of the heat supply is a geothermal probe field instead of ambient air, up to 100 tons of CO_2 can be saved over a period of 25 years. Solar regeneration not only enables a reduction of length or number of the borehole heat exchangers, but also generally ensures a more sustainable operation of the system. For this purpose, comparative temperature cross sections of probe fields with 12 probes resulting from the TRNSYS simulations are shown in Figure 6.

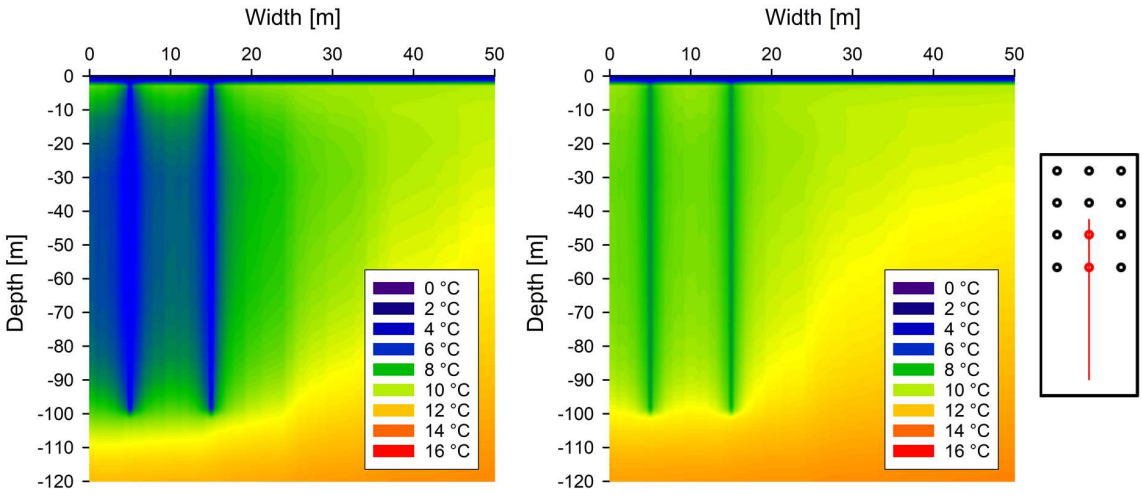

Fig. 6: Vertical temperature cross sections of probe fields with 12 probes after an operating time of 25 years (31. December): without solar regeneration (left) and with solar regeneration (120 m² collector surface, right). Shown are the two probes highlighted in the schematic on the far right.

In contrast to the reference system, the temperature in the ground is not influenced so strongly in the long term in case of solar regeneration: the soil cools down more slowly and a stationary level is reached after only a few years. Without regeneration the ground continues to cool down even after 25 years of operation. At the same time, the robustness of the system can be increased by solar regeneration, especially for undersized borehole heat exchangers. These results are also in line with the findings of previous ISFH projects (Bertram et al., 2014) and further studies, e.g. by Persdorf et al. (2015). Additional simulations show that the probe spacing can be halved in case of solar regeneration without compromising the system performance, since regeneration significantly reduces the mutual interaction between the probes. Figure 7 compares the change of the seasonal performance factor over the operating time of 25 years for different distances of the probes in the field with and without solar regeneration. On the left side a field with 9 probes and on the right side one with 16 probes.

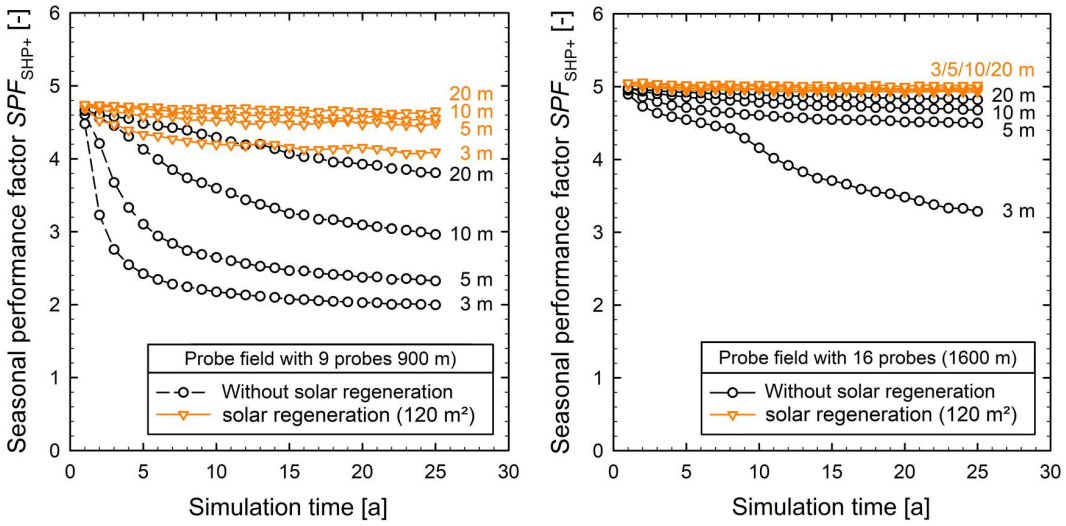

Fig. 7: Change of the seasonal performance factor over the operating time of 25 years for different distances of the probes in the field with and without solar regeneration: A probe field with 9 probes (left) and a probe field with 16 probes (right)

The efficiency of the system with solar regeneration is not significantly affected by reducing the distance from 10 m to 5 m, even with tightly dimensioned probe fields (9 probes). The required surface area of the field can therefore be significantly reduced by saving probes or probe length and reducing the distance between the probes. For the described system, for example, the required surface area for the probe field can be reduced from 900 m² (16 probes; 10 m distance) to 150 m² (12 probes; 5 m distance). This comes with the same efficiency and higher robustness, and corresponds to an area reduction of 83.3%. The effect significantly extends the range of applications of efficient heat pump systems with borehole heat exchangers, which usually require a lot of space. Another possible application for solar regeneration with steel sandwich elements is the replacement of an old heat pump with a more efficient new unit. Here, the existing geothermal heat source may be undersized, so that regeneration through the solar panels offers the possibility to keep the existing plant operational.

The results of the variation of the solar absorptance (52.8 % to 91.3 %) of cover plates with different colors are shown in Figure 8. A low absorptance only has an impact in undersized systems. With a large collector surface (120 m²), only the lightest shade of gray (RAL 9006) leads to a minor reduction in efficiency. This means that different colors with higher absorptance, such as dark blue, dark green, dark red, dark gray and black, can be used for the solar panels without significantly affecting the system performance, thus ensuring architects a very high degree of design freedom.

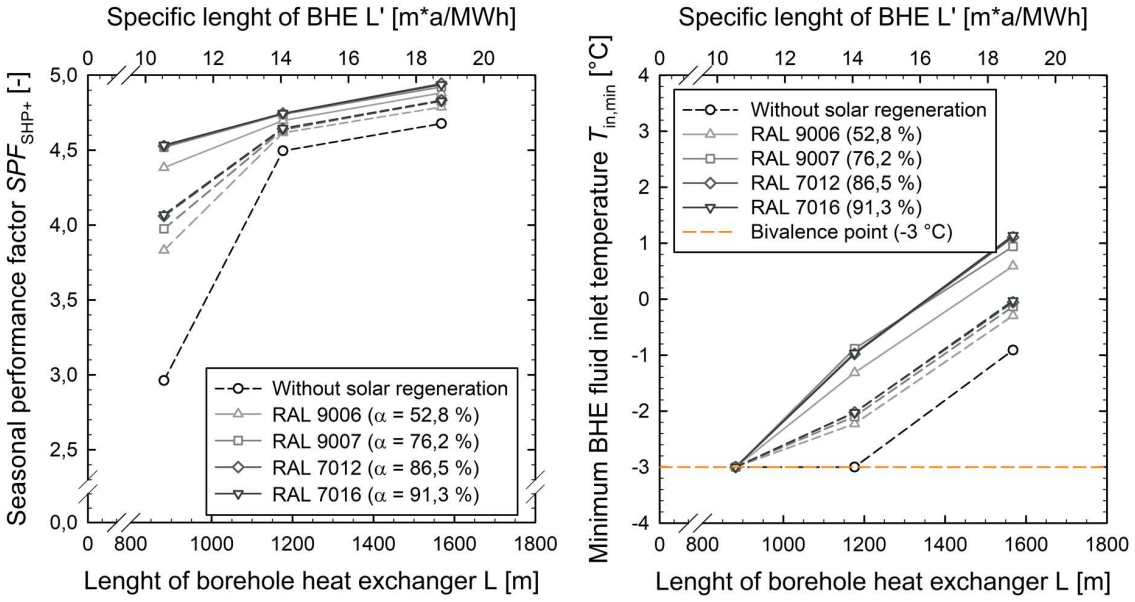

Fig. 8: Seasonal performance factor (left) and minimum fluid inlet temperature into the probe field for modules with different solar absorptance and collector surfaces of 60 m² (striated) and 120 m² (continuous), after an operating time of 25 years

4. Cost analysis

The economic evaluation of the systems is based on a simplified approach of the levelized cost of heat (LCoH) methodology, as defined by Louvet et al. (2018). Corporate taxes, an annual depreciation or any residual values are not taken into account. The discount rate is set to 0% and no subsidies are used. This simplifies the formula for the heat production costs as follows:

$$LCoH = \frac{I_0 + \sum_{t=1}^{T} C_t}{\sum_{t=1}^{T} E_t} \quad \text{(eq. 3)}$$

- $LCoH$: levelized cost of heat [€/kWh]
- I_0: initial investment [€]
- C_t: yearly operation and maintenance costs [€]
- E_t: yearly energy consumption [kWh]
- t: year
- T: evaluation period in years

The annual maintenance M_t and the annual operation costs O_t are summarized in the running costs C_t:

$$C_t = O_t + M_t \quad \text{(eq. 4)}$$

These two costs are calculated and handled separately for the following studies.

4.1. Boundary conditions

The investment costs of the investigated systems are shown in Table 2. All costs are calculated without value added tax and are based on estimates and mean values from offers obtained from manufacturer and planner.

Tab. 2: Investment costs of the two reference systems and the system with solar regeneration

Probe length	**600 m**	**900 m**	**1200 m**	**1600 m**
System configuration	**Investment costs**			
Reference HP+ BHE	70 000 €	87 500 €	105 000 €	128 500 €
Reference air-to-water HP	45 000 €			
Solar regeneration 120 m²	77 000 €	94 500 €	112 000 €	135 500 €

It is noticeable that the investment costs for the probe field are a large part of the investment costs. For the annual maintenance costs, a conservative value is determined in accordance with VDI 2067 (2012), which corresponds to 3% of the respective investment costs. The electricity price, which is decisive for the operation-related costs, is assumed to be 22.2 €ct/kWh with an annual price increase of 3%. These values correspond to the current price level for smaller businesses with an annual electricity demand of up to 100,000 kWh and an average price change rate of the last 10 years. The evaluation period is set to 25 years, analogously to the system simulations. The lifetime of the main components is approximately in this range. A replacement of hydraulic pumps is included in the maintenance costs. Shorter evaluation periods, which are common in industrial and commercial applications, enormously favor the investment-friendly system with an air-to-water heat pump.

4.2 Results

The estimation for all three investigated systems comes to comparable levelized cost of heat for a borehole heat exchanger with a length of 1200 m (12 probes) (see Figure 9, left). The use of solar-thermally activated sandwich elements can save approx. 10,000 € in investment costs. This result is achieved by saving 25 to 30% of the borehole heat exchangers and, at the same time, making an additional investment in the solar façade. The reference system with an air-to-water heat pump is significantly less expensive in investment, but has similarly high cost of heat due to the higher power consumption during operation and the associated electricity costs. The levelized cost of heat in €ct/kWh are shown in Figure 9 on the left side. A more detailed breakdown of the investment, maintenance and operating costs for selected scenarios is shown on the right side of the figure. The graph illustrates clearly that a higher investment is associated with a higher efficiency of the system and thus lower operating costs.

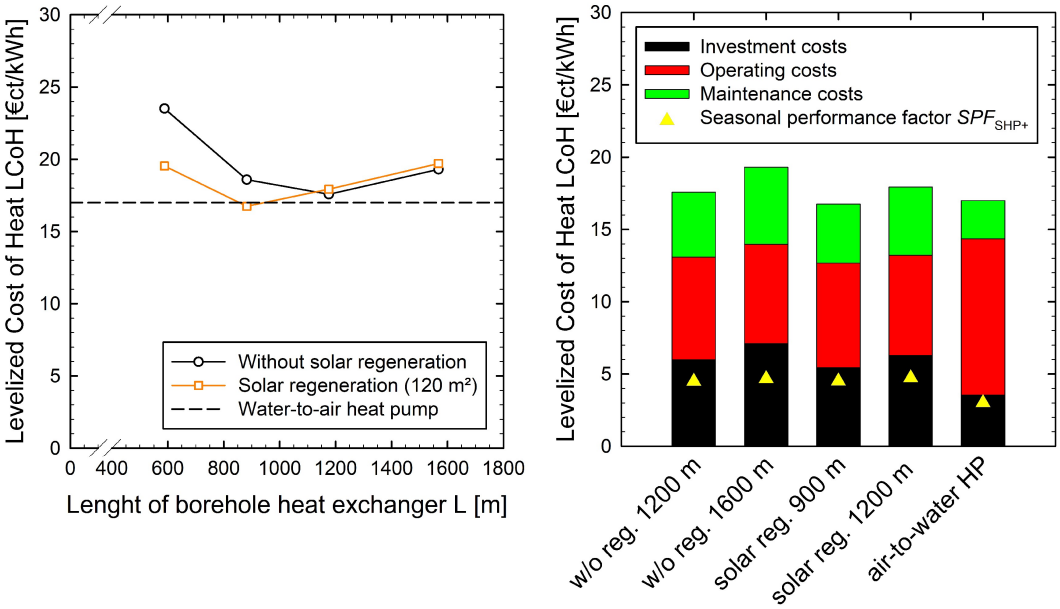

Fig. 9: Levelized cost of heat in €ct/kWh (left) and detailed representation of the individual cost parameters (right)

These results are not fully reliable due to uncertainties regarding the investment costs and the development of electricity prices. Therefore, we carried out a sensitivity analysis to investigate which parameters influence the levelized cost of heat to what extent. Figure 10 shows the impact of individual cost parameters for a ground-coupled heat pump system with solar regeneration (left) and a system with an air-to-water heat pump (right).

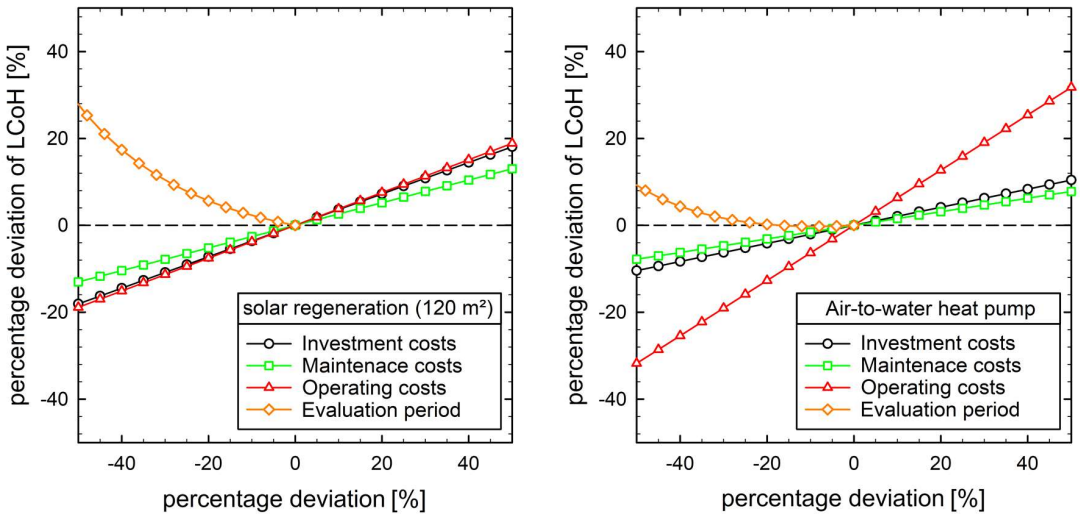

Fig. 9: Influence of individual cost parameters and the evaluation period on the levelized costs of heat for the system with 1200 m solar regenerated borehole heat exchangers (left) and the air-to-water heat pump system (right)

The individual cost parameters have a very different influence on the two systems, as expected. Due to the different investment costs, the evaluation period has a much larger impact on the ground-coupled system. The air-to-water heat pump system, on the other hand, is mainly influenced by the operation costs.

5. Summary

This paper presents the behavior of solar-activated steel sandwich elements in low-temperature heat supply systems with ground-coupled heat pumps for commercial and industrial applications. The simulation results show that by using the solar energy gained from façades to regenerate the borehole heat exchanger, the length or the number of the boreholes can be reduced by 25 % to 30 %. In addition, the distance between the individual probes can be significantly reduced. Thus more than 80 % of the required area of the probe field can be saved. Regeneration can also ensure a more sustainable operation of the systems and make them more robust against insufficient dimensioning. When planning solar-thermally activated steel sandwich façades, a great design freedom is given with regards to the color of the panels. The selection of color shades with a solar absorptance above 76 % is enough to ensure the maximum efficiency of solar regeneration. Besides different shades of grey, also red, green or blue coatings can thus be taken into consideration by architects.

The levelized cost of heat of the solar-assisted system are comparable to those of the reference systems. However, the use of steel sandwich elements can slightly reduce the investment by reducing the size of the geothermal heat exchanger. The respective costs of a reference system with an air-to-water heat pump are also in the same range. But this comes with 30% less efficiency and therefore more electricity is required to cover the heat demand.

6. Acknowledgement

The AiF research project "Building-integrated solar steel sandwich elements with mineral wool core for industrial and commercial construction“ underlying this publication is funded by the state of Lower Saxony and the Federal Ministry of Economic Affairs and Energy under the reference number 19520N following a decision of the German Bundestag. The work is carried out in cooperation with the Dortmund University of Applied Sciences and Arts, Department of Architecture and Metal Construction and the Research Association for Steel Application (FOSTA). The authors thank for the support as well as for the fruitful cooperation with the project partners. The responsibility for the content of this publication lies exclusively with the authors.

7. References

BAuA, 2018. Technical rules for workplaces – room temperature - ASR A3.5, 2010, modified 2018

Bertram, E., 2014. Solar Assisted Heat Pump Systems with Ground Heat Exchanger – Simulation Studies in: Energy Procedia Vol. 48, pp 505-514

DIN, 2018. DIN V 18599:2018-12, Energy efficiency of buildings - Calculation of the net, final and primary energy demand for heating, cooling, ventilation, domestic hot water and lighting. Beuth Verlag, Berlin

EEWärmeG, 2008. Renewable Energies Heating Act. Beuth Verlag, Berlin

EnEV, 2016. EnEV 2014, Energy Saving Directive, status as of 2016

Feldmann, M., Kuhnhenne, M., Pyschny, D., Brieden, M., Hachul, H., Bach, J., Rößling, H., Rexroth, S., Deininger, F., Morana, R., Görner, R., Ummenhofer, T., Misiek, T., Krüger, H., Fauth C., 2014. Mehrdimensionale energieoptimierte Gebäudehüllen in Stahlleichtbauweise für den Industrie- und Gewerbebau, final report of the AiF project P880 / IGF-Nr. 16936. Düsseldorf

Föste, S., 2013. Flachkollektor mit selektiv beschichteter Zweischeibenverglasung, thesis (in german). Hannover

Hadorn, J.-C., 2015. Solar and Heat Pump Systems for Residential Buildings. Final report, IEA SHC TASK 44. Ernst & Sohn, Berlin

ISO, 2018. ISO 9806:2018-04. Solar energy – Solar thermal collectors – Test methods, German version. Beuth Verlag, Berlin

Louvet, Y., Fischer, S., Furbo, S., Giovannetti, F., Mauthner, F., Mugnier, D., Philippen, D., 2018. Guideline for levelized cost of heat (LCOH) calculations for solar thermal applications. Info sheet A.2, IEA SHC TASK 44

Malenković, I., Pärisch, P., Eicher, S., Bony, J., Hartl, M., 2013. Definition of Main System Boundaries and Performance Figures for Reporting on SHP Systems. Technical report, IEA SHC TASK 54

Meteonorm, 2015. Handbook Part I & II (Version 7.1), Bern

Oschatz, B., Rosenkranz, J., Weber, K., 2015. Leitfaden zur Planung neuer Hallengebäude nach Energieeinsparverordnung EnEV 2014 und Erneuerbare-Energien-Wärmegesetz 2011. Figawa, Köln

Persdorf, P., Ruesch, F., Haller, M. Y., 2015. RegenOpt, final report. Zürich

SIA, 2010. SIA 384/6:2010, Erdwärmesonden. Zürich

Transsolar Energietechnik, 2012. TRNSYS Version 17.01

VDI, 2012. VDI 2067-1:2012-09, Economic efficiency of building installations - Fundamentals and economic calculation. Beuth Verlag, Berlin

VDI, 2019. VDI 4640-2:2019-06, Thermal use of the underground - ground source heat pump systems. Beuth Verlag, Berlin

Weiland, F., Kirchner, M., Rensinghoff, V., Giovannetti, F., Kastner, O., Ridder, D., Tekinbas, Y., Hachul, H., 2019. Performance assessment of solar thermally activated steel sandwich panels with mineral wool core for industrial and commercial buildings. J. Phys. Conf. Ser. 1343 012098